http://dx.doi.org/10.5012/bkcs.2012.33.11.3576

Influence of SiO_2 Capping and Annealing on the Luminescence Properties of Larva-Like GaS Nanostructures

Hyunsu Kim, Changhyun Jin, Sunghoon Park, and Chongmu Lee*

*Department of Materials science and Engineering, Inha University, Incheon 402-751, Korea. *E-mail: cmlee@inha.ac.kr*
Received June 27, 2012, Accepted August 1, 2012

Larva-like GaS nanostructures synthesized by the thermal evaporation of Ga metals and S powders were coated with SiO_2 by the sputtering technique. Transmission electron microscopy and X-ray diffraction analyses revealed that the cores and shells of the GaS-core/SiO_2-shell larva-like nanostructures were single crystal wurtzite-type hexagonal structured-GaS and amorphous SiO_2, respectively. Photoluminescence (PL) measurements at room temperature showed that the passivation of the larva-like GaS nanostructures was successfully achieved with SiO_2 without nearly harming the major emission from the wires. However, subsequent thermal annealing treatment was found to be undesirable owing to the degradation of their emission in intensity.

Key Words : Nanostructures, GaS, SiO_2, Core-shell structure, Photoluminescence

Introduction

Gallium sulfide (GaS) is a wide bandgap semiconductor with layered structures of particular interest owing to its highly anisotropic structural, electrical, optical, and mechanical properties. These properties make it a promising candidate for applications in photoelectric devices, electrical sensors, and nonlinear optical applications.[1-5] Hexagonal GaS, with direct wide band gap of 3.05 eV and indirect band gap of 2.5 eV, is more useful for optoelectronic applications.[1] GaS crystallizes in a layered structure with a double layer of nonmetal atoms, consisting of S-Ga-Ga-S sheets, stacking along the c axis, having intralayer van der Walls bonding and interlayer covalent bonding and is structurally similar to graphite.[2-4] Particularly regarding the optical properties, doped GaS is a promising material for the fabrication of near-blue-light emitting devices.[5] The GaS thin films deposited on the GaAs substrate are reported to be able to enhance the photoluminescence yield of GaAs by 2 orders of magnitude.[6]

In recent years, one-dimensional (1D) nanostructures have been extensively investigated due to their interesting properties and potential applications in electronics and optoelectronics.[7,8] There are a few reports on synthesis of GaS nanotubes and thin films fabricated by molecular organic chemical vapor deposition (MOCVD) and molecular beam epitaxy (MBE). However, thermal evaporation may be a more attractive technique in synthesizing GaS nanostructures with an advantage of synthesizing various forms of GaS nanostructures depending on the substrate temperature at lower temperatures compared to other techniques. Recently, Panda *et al.* synthesized short GaS nanobelts using catalyst-assisted thermal evaporation method.[9] Shen *et al.* reported the controlled synthesis of high quality GaS nanostructures on a large scale using a simple catalyst-free thermal evaporation method.[8] The morphologies (thin nanowires, nanobelts, zigzag nanobelts, microbelts, hexagonal microplates) and compositions of the GaS products (heterostructured nanobelts) were controlled by substrate temperature as well as evaporation source.

It is essential to passivate 1D nanostructures with insulating materials to protect them from contamination and oxidation as well as to avoid crosstalking between the building blocks of complex nanoscale circuits.[11,12] Passivation also offers many advantages such as substantial reduction of surface states, prevention of the surface from adsorption of unwanted species, prevention of unnecessary charge injection, and partial screening of the external fields.[13,14] In particular, passivation of nanostructures is required in the fabrication of field effect transistors and sensor devices based on nanostructures. Silicon dioxide (SiO_2) is known as one of the most suitable insulating material for nanostructure passivation owing to its excellent insulating property, low dielectric constant, and high mechanical strength as well as compatibility with other materials widely used in integrated circuits (IC) fabrication.[15] SiO_2 is also optically transparent for light absorption or emission of semiconductor nanostructures, resulting in minimal destruction of their intrinsic optical properties such as photoluminescence (PL).[16,17] On the other hand, various techniques have been reported to be used to form SiO_2 passivation layers on the nanostructure cores. These techniques include sol-gel processes, thermal heating, solution-based methods, CVD, atomic layer deposition (ALD), and sputtering.[18-25] Of these techniques, the sol-gel process and solution-based wet processes are prone to contamination. SiO_2 cannot be grown on the GaS nanostructures by thermal heating because no silicon source is contained in the GaS nanostructures. It is difficult to optimize the ALD process condition for SiO_2 coating using a silicon precursor such as SiH_4, Si_2Cl_2, or $SiCl_4$ and an oxygen precursor such as O_2 or N_2O because of a narrow process window. Therefore, among the above mentioned techniques for the formation of SiO_2 passivation layers, sputtering is the simplest clean technique which can be used for coating SiO_2 onto larva-like

GaS nanostructures. In this paper, we report fabrication of GaS-core/SiO_2-shell larva-like nanostructures by using a two-step process: thermal evaporation of Ga metals and S powders and sputter-deposition of SiO_2. We also investigated the influence of SiO_2 coating on the photoluminescence properties of larva-like GaS nanostructures and thermal annealing on the PL properties of core-shell nanowires and the origin of the change in the PL emission intensity by annealing.

Experimental

GaS nanostructures were synthesized by the thermal evaporation technique based on a vapor-liquid-solid (VLS) mechanism. The thermal evaporation process was carried out in a conventional horizontal tube furnace. Two alumina boats with a length of 4 cm and a diameter of 1.5 cm containing sulfur powders and several pieces of bulk Ga metal were placed in the downstream direction at the center of the quartz tube and a piece of P-type Si (100) wafer used as the substrate for the deposition of GaS nanostructures were placed about 12 cm apart from the alumina boat containing Ga metals in the downstream direction. After the arrangement of the substrates, the tube was pumped down to 0.8 Torr using a rotary pump. High purity argon gas was introduced into the tube with a flow rate of 100 cc/min throughout the whole synthesis process. The temperature of the evaporation sources (Ga metals and S powders) in the furnace was increased to 800 °C at a heating rate of 30 °C/min. The substrate temperature during the evaporation process was measured to be ~700 °C. After maintaining for 1 h. the furnace was cooled to room temperature to take out the products. During the synthesis process, the substrate temperature was monitored using a thermocouple.

Next, coating of the nanostructures with SiO_2 was carried out by sputtering. The sputter-deposition was done at room temperature using a 99.999% SiO_2 target in a radio-frequency (rf) magnetron sputtering system. After the sputtering chamber was evacuated to 1×10^{-6} Torr using a turbomolecular pump backed by a rotary pump. Ar was provided at a flow rate of 20 cc/min. Depositions were carried out at room temperature for 20 min. The system pressure and the rf sputtering power were 1.7×10^{-2} Torr and 100 W, respectively. Subsequently, the prepared SiO_2-coated GaS nanostructure samples were optionally annealed in an O_2 atmosphere at 650 °C for 30 min to see the influence of annealing on the PL properties of the core-shell nanostructures.

The morphology and size of the final products were examined by using scanning electron microscopy (SEM, Hitachi S-4200). High resolution transmission electron microscopy (HRTEM) and selected area electron diffraction (SAED) were carried out on Philips CM-200 electron microscope at an acceleration voltage of 200 kV. The samples used for characterization were dispersed in absolute ethanol and ultrasonicated before TEM observations. Glancing angle (0.5°) X-ray diffraction (XRD) analysis was performed using a Rigaku DMAX 2500 X-ray diffractometer with Cu-Kα radiation with an incident angle of 0.5° to investigate the phases of the obtained products. The compositional analysis was done by using energy dispersive X-ray spectroscope (EDXS) installed in the TEM. The PL measurement was carried out at room temperature by using a He-Cd laser (Kimon, 1 K, Japan) line (325 nm, 55 mW) as the excitation source.

Results and Discussion

Figure 1(a) shows the SEM image of the as-synthesized SiO_2-coated GaS nanostructures. The nanostructures look like the grains of steamed rice or larvas. Figure 1(a) shows that the widths and lengths of the nanostructures ranged from 100 to 200 nm and from 200 to 700 nm, respectively. A statistical analysis of many SEM images revealed that the diameters of the as-synthesized SiO_2-coated GaS nanostructures ranged from 100 to 400 nm and that the maximum of the diameter distribution was at 150 nm (Fig. 1(b)). The spherical droplets or particles were observed at the tips of many nanostructures (Fig. 1(a), Inset) indicating the VLS growth of the nanostructures. The XRD patterns of the as-

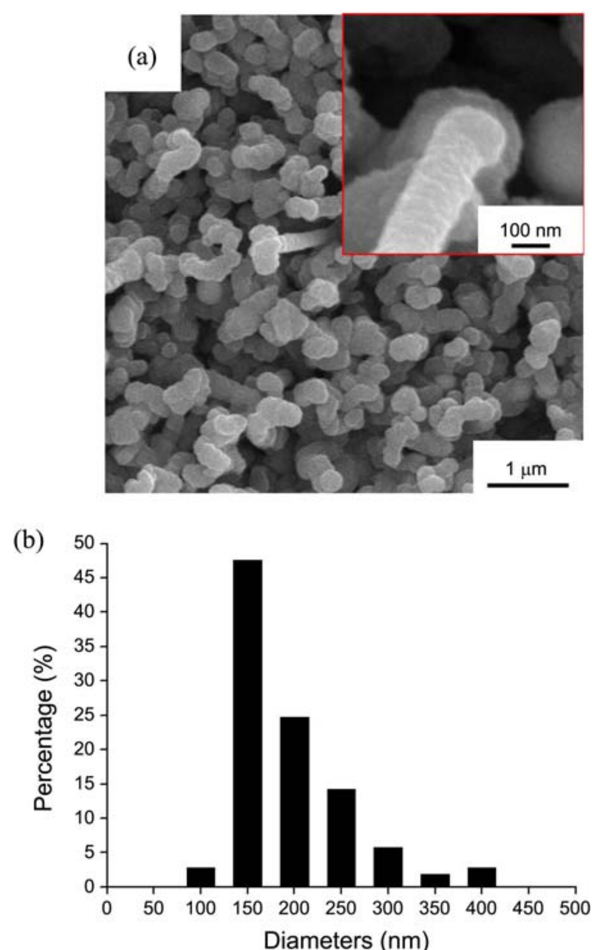

Figure 1. SEM images of the (a) as-synthesized and GaS-core/SiO_2-shell nanostructures. Inset is the enlarged image of a typical nanowire, (b) Distribution of the diameters of the SiO_2-coated ZnO nanostructures.

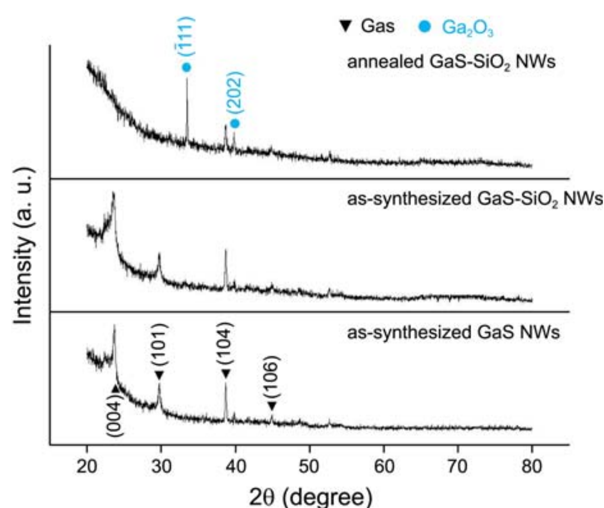

Figure 2. Glancing angle XRD patterns of the SiO_2-coated ZnO nanostructures.

synthesized and annealed SiO_2-coated GaS nanostructures along with that of as-synthesized GaS nanostructures are shown in Figure 2. In both of the SiO_2-coated and uncoated GaS nanostructures four peaks characteristic of wurtzite-type hexagonal GaS ($P6_3mc$, a = 0.3587 nm, c = 1.5492 nm) were identified, which were indexed as the (004), (101), (104), (106) reflections from GaS. On the other hand, no reflection peaks of SiO_2 were observable, suggesting that the SiO_2 shells are amorphous. In contrast, Ga_2O_3 ($\bar{1}$11) and (202) reflections instead of the GaS reflection peaks were observed, indicating that Ga_2O_3 has been transformed to GaS by the annealing process.

Figure 3(a) is the low-magnification TEM image of a typical SiO_2-coated GaS nanostructure clearly showing two segments: a thicker core ~80 nm thick and two thinner coating layers with an average thickness of 30-50 nm on both sides of the core. The high resolution TEM (HRTEM) image of the interfacial area of the core and shell of a typical SiO_2-coated GaS nanostructure and the associated selected area electron diffraction (SAED) pattern taken along the [0001] zone axis are shown in Figures 3(b) and (c). The resolved spacing between the two parallel neighboring fringes is about 0.38 nm, corresponding to the (004) lattice plane of wurtzite GaS. Both the HRTEM image and the SAED pattern indicate that the GaS core is wurtzite-type GaS. In contrast, neither a fringe pattern in the shell layer of the HRTEM image nor the spotty (or ring) pattern for crystalline SiO_2 in the SAED pattern is observed, suggesting that the SiO_2 shell is amorphous. The EDX spectrum for the particle (Fig. 1(d)) shows that the particle comprises Au as well as Ga, S, Si, and O. The Cu detected in the spectrum was not used as a catalyst but as a conductor for TEM sample preparation. These results suggest that the GaS nanostructures were grown through the conventional VLS mechanism in which a liquid Au catalyst droplet was located at the growth front of each wire.[26]

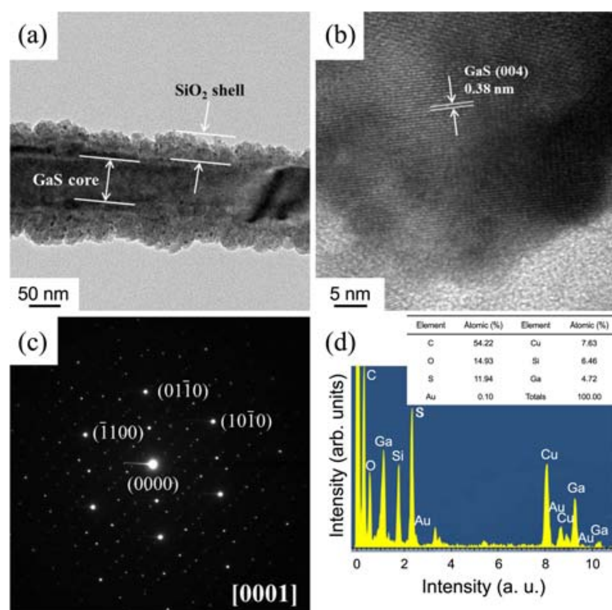

Figure 3. (a) Low-magnification TEM image of a typical SiO_2-coated GaS nanostructure, (b) HRTEM image of a region near the interface of the core and the shell in a typical GaS-core/SiO_2-shell nanostructure, and (c) corresponding SAED pattern, (d) EDX spectrum of GaS-core/SiO_2-shell nanostructures.

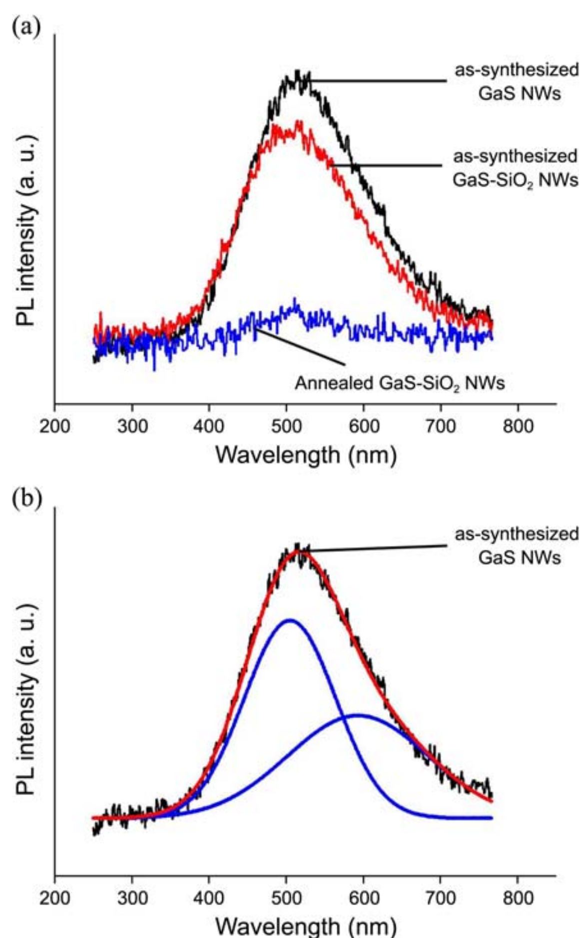

Figure 4. (a) PL spectra of as-synthesized GaS nanostructures, and as-synthesized and annealed GaS-core/SiO_2-shell nanostructures and (b) Gaussian fitting of the PL spectra of the as-synthesized GaS nanostructures.

Room-temperature PL measurements were carried out. Figure 4(a) displays the PL spectra of the as-synthesized and annealed GaS nanostructures and as-synthesized and annealed SiO_2-coated GaS nanostructures, *i.e.*, GaS-core/SiO_2-shell nanostructures. The GaS nanostructure sample exhibits a relatively strong green emission at approximately 510 nm. Gaussian fitting (Fig. 4(b)) revealed that the major emission band consisted of the emission band centered at approximately 500 nm and that centered at approximately 610 nm. Aydinli *et al.* reported three broad PL bands centered at 558, 614, and 780 nm at 9 K in the PL spectrum of well aligned GaS horn-like nanostructures.[27] The origin of the emission may be attributed mainly to structural defects such as S interstitials, Ga vacancies, stacking defects, and surface states.[27] The orange emission peak at 610 nm is in agreement with the emission peak at 614 nm that Aydinli *et al.* reported. On the other hand, the green emission from GaS nanostructures has not been reported before. There are two possibilities regarding the origin of the green emission at 500 nm observed in this study. One possibility is that it is a band-to-band emission considering the band gap energy of GaS. The indirect band gap energy, 2.5 eV of GaS corresponds to 496 nm, which is in good agreement with the green peak in this study (500 nm). The other possibility is that it is also associated with Ga vacancy- or S interstitial-related defects which can easily form recombination centers. The probability of indirect transition occurring in the GaS nanostructures synthesized in this study is low because the nanostructures were not doped with any other impurities. Therefore, it is more reasonable to assume that the green emission also originates from the structural defects. The radiative recombination of electrons from the conduction band minimum by holes from deep acceptor centers such as the aforementioned structural defects might produce PL emissions in the GaS nanostructures.[28]

In contrast to the GaS nanostructures, the GaS-core/SiO_2-shell nanostructures exhibit a slightly weaker green emission band centered at approximately 510 nm. In other words, the green emission was slightly decreased by coating the GaS nanostructures with SiO_2. This decrease in the PL emission intensity might be attributed to the light absorption by the SiO_2 shell layer. Incident light to the nanostructures and the light emitted by the nanostructures must pass the SiO_2 shell layer. Therefore, the final intensities of the PL emissions must be influenced by the transmittance of the shell layer. It is assumed that the intensity of the light passing through the SiO_2 shell layer is somewhat lower than that of the light before entering the shell layer because the transparency of the thin SiO_2 layer is not perfect. It is important that passivation of the GaS nanostructures could be achieved with SiO_2 without nearly harming the intensity of the major emission from the nanostructures.

On the other hand, the green emission of the GaS-core/SiO_2-shell nanostructures was decreased in intensity considerably by thermal annealing, which might be attributed to the following two sources:

1) Consumption of the GaS phase and formation of a Ga_2O_3 phase as a result of the following reaction:[29]

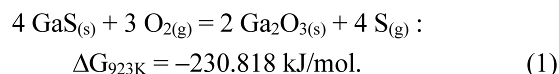

$$4\ GaS_{(s)} + 3\ O_{2(g)} = 2\ Ga_2O_{3(s)} + 4\ S_{(g)} : \quad \Delta G_{923K} = -230.818\ \text{kJ/mol}. \tag{1}$$

Because the SiO_2 shell layers are as thin as 30-50 nm and the mean diffusion length of O_2 in SiO_2 at 650 °C for 30 min, $x = (Dt)^{1/2} = \sim 1.0 \times 10^5$ nm because the diffusion coefficient of O_2 in SiO_2, $D_{923K} = \sim 6.0 \times 10^{-8}$ cm/sec[30] and t = 1,800 sec, O_2 molecules can diffuse very easily through the SiO_2 shell layer to reach the GaS-SiO_2 interface and to react with GaS during the annealing process. However, as written above XRD analyses revealed that most of the GaS cores had transformed to Ga_2O_3 during the annealing process. The PL spectrum of the as-synthesized Ga_2O_3 nanowires is commonly characterized by an emission band centered at approximately 510 nm in the green region.[31,32] This green emission was reported to be associated with the vacancies in the Ga_2O_3 nanostructures, such as gallium (Ga) vacancies, oxygen (O) vacancies[31] and Ga-O vacancy pairs.[32] Therefore, it is not clear if the small emission peak of the GaS-core/SiO_2-shell nanostructures is from the remaining GaS phase or from the newly formed Ga_2O_3 phase. Anyhow, considering the lower intensity of the green emission from the annealed core-shell nanostructures than the as-synthesized core-shell nanostructures we may well assume that the emission intensity of the Ga_2O_3 phase is lower than that of the GaS phase.

2) An increase in the concentration of deep levels such as O interstitials in the GaS cores due to the inflow of O atoms from the O_2 atmosphere into the cores during the annealing process. Even in the case that the O atoms from the O_2 atmosphere did not react with GaS, it would stay as O interstitials which could also be a source for the grren emission.

The above experimental results indicate that thermal annealing treatment is not desirable after capping the GaS nanostructures. In addition, the electrical resistivities of the SiO_2-coated and uncoated *i.e.*, as-synthesized GaS nanostructures measured using a four-point probe technique were 1.7×10^{12} Ω cm and 7.84×10^8 Ω cm, respectively. This result verifies that GaS nanostructures can be passivated by SiO_2 coating in terms of electrical insulation.

Conclusions

Larva-like GaS-core/SiO_2-shell nanostructures were synthesized by a two step process: the thermal evaporation of Ga metal and S powders and the sputter-deposition of SiO_2. The GaS cores and the SiO_2 shells of the nanostructures were single crystal wurtzite-type GaS and amorphous SiO_2, respectively. The as-synthesised GaS nanostructures showed a relatively strong green emission band centered at approximately 510 nm. Passivation of the GaS nanostructures could be achieved with SiO_2 without nearly harming the intensity of the major emission from the nanostructures. Thermal annealing treatment was, however, found to be undesirable owing to the degradation of the emission in intensity.

Acknowledgments. This work was supported by the Korea Research Foundation through 'the 2010 Core Research Program'.

References

1. Gasanly, N. M.; Aydinli, A.; Ozkan, H.; Kocabas, C. *Solid State Commun.* **2000**, *116*, 147.
2. Khler, Th.; Frauenheim, Th.; Hajnal, Z.; Seifert, G. *Phys. Rev. B* **2004**, *69*, 193403.
3. Lieth, R. M. A. *Preparation and Crystal Growth of Materials with Layered Structures*; D. Reidel Publishing: Dordrecht, The Netherlands, 1977.
4. Gautam, U. K.; Vivekchand, S. R. C.; Govindaraj, A.; Kulkarni, G. U.; Selvi, N. R.; Rao, C. N. R. *J. Am. Chem. Soc.* **2005**, *127*, 3658.
5. Aono, T.; Kase, K.; Kinoshita, A. *J. Appl. Phys.* **1993**, *74*, 2818.
6. Xin, Q. S.; Conrad, S.; Zhu, X. Y. *Appl. Phys. Lett.* **1996**, *69*, 1244.
7. Shen, G. Z.; Bando, Y.; Liu, B.; Tang, C.; Huang, Q.; Golberg, D. *Chem. Eur. J.* **2006**, *12*, 2987.
8. Kim, H. W.; Kim, N. H. *Adv. Appl. Ceram.* **2006**, *105*, 84.
9. Panda, S. K.; Datta, A.; Sinha, G.; Chaudhuri, S.; Chavan, P. G.; Patil, S. S.; More, M. A.; Joag, D. S. *J. Phys. Chem. C* **2008**, *112*, 6240.
10. Chen, C.; Guo, H. B.; Shapiro, I. P.; Peng, H.; Zhao, X. F.; Xiao, P.; Gong, S. K. *Adv. Appl. Ceram.* **2010**, *109*, 95.
11. Lauhon, L. J.; Gudiksen, M. S.; Wang, D.; Lieber, C. M. *Nature* **2002**, *420*, 57.
12. Morales, A. M.; Lieber, C. M. *Science* **1998**, *279*, 208.
13. Li, Y. B.; Bando, Y.; Goldberg, D.; Uemura, Y. *Appl. Phys. Lett.* **2003**, *83*, 3999.
14. Liang, X.; Tan, S.; Tang, Z.; Kotov, N. A. *Langmuir* **2004**, *20*, 1016.
15. Bartzsch, H.; Glâ, D.; Bcher, B.; Frach, P.; Goedicke, K. *Surf. Coat. Technol.* **2003**, *174-175*, 774.
16. Pan, A.; Wang, S.; Liu, R.; Li, C.; Zou, B. *Small* **2005**, *1*, 1058.
17. Chang, Y.; Wang, M.; Chen, X.; Ni, S.; Qiang, W. *Solid State Comm.* **2007**, *142*, 295.
18. Kim, N. H.; Kim, H. W.; Seoul, C.; Lee, C. *Mater. Sci. Eng. B* **2004**, *111*, 131.
19. Park, S.; Kim, H.; Lee, J. W.; Kim, H. W.; Lee, C. *J. Kor. Phys. Soc.* **2008**, *53*, 657.
20. Jun, J.; Jin, C.; Kim, H.; Kang, J.; Lee, C. *Appl. Phys. A* **2009**, *96*, 813.
21. Park, S.; Jun, J.; Kim, H. W.; Lee, C. *Solid State Comm.* **2009**, *149*, 315.
22. Jun, J.; Jin, C.; Kim, H.; Park, S.; Lee, C. *Appl. Surf. Sci.* **2009**, *255*, 8544.
23. Jin, C.; Kim, H.; Kim, H. W.; Lee, C. *J. Luminescence* **2010**, *130*, 516.
24. Jin, C.; Kim, H.; Baek, K.; Kim, H. W.; Lee, C. *Cryst. Res. Technol.* **2010**, *45*, 199.
25. Wang, Y.; Tang, Z.; Liang, X.; Liz-Marzán, L. M.; Kotov, N. A. *Nano Lett.* **2004**, *4*, 225.
26. Wagner, R. S.; Ellis, W. C. *Appl. Phys. Lett.* **1964**, *4*, 89.
27. Aydinli, A.; Gasanly, N. M. Goksen, *J. Appl. Phys.* **2000**, *88*, 7144.
28. Shigetomi, S.; Ikari, T. J. *Appl. Phys.* **2007**, *102*, 033701.
29. Barin, I. *Thermochemical Data of Pure Substances*, 3rd Ed.; VCH: Weinheim: Basel, 1995.
30. Meek, R. L. *J. Amer. Cer. Soc.* **1973**, *56*, 341.
31. Harwig, T.; Kellendouk, F. *J. Solid State Chem.* **1978**, *24*, 255.
32. Vasil'tsiv, V. I.; Zakharko, Ya. M.; Prim, Ya. I. *Ukr. Fiz. Zh.* **1988**, *33*, 255.